UNIVERSITY OF BIRMINGHAM
University of Birmingham Research at Birmingham

# Effect of pulse frequency on the one-step preparation of superhydrophobic surface by pulse electrodeposition

Jiang, Shuzhen; Guo, Zhongning; Deng, Yu; Dong, Hanshan; Li, Xiaoying; Liu, Jiangwen

*DOI:*
10.1016/j.apsusc.2018.07.120

*License:*
Creative Commons: Attribution-NonCommercial-NoDerivs (CC BY-NC-ND)

*Document Version*
Peer reviewed version

*Citation for published version (Harvard):*
Jiang, S, Guo, Z, Deng, Y, Dong, H, Li, X & Liu, J 2018, 'Effect of pulse frequency on the one-step preparation of superhydrophobic surface by pulse electrodeposition', *Applied Surface Science*, vol. 458, pp. 603-611. https://doi.org/10.1016/j.apsusc.2018.07.120

Link to publication on Research at Birmingham portal

**General rights**
Unless a licence is specified above, all rights (including copyright and moral rights) in this document are retained by the authors and/or the copyright holders. The express permission of the copyright holder must be obtained for any use of this material other than for purposes permitted by law.

•Users may freely distribute the URL that is used to identify this publication.
•Users may download and/or print one copy of the publication from the University of Birmingham research portal for the purpose of private study or non-commercial research.
•User may use extracts from the document in line with the concept of 'fair dealing' under the Copyright, Designs and Patents Act 1988 (?)
•Users may not further distribute the material nor use it for the purposes of commercial gain.

Where a licence is displayed above, please note the terms and conditions of the licence govern your use of this document.

When citing, please reference the published version.

**Take down policy**
While the University of Birmingham exercises care and attention in making items available there are rare occasions when an item has been uploaded in error or has been deemed to be commercially or otherwise sensitive.

If you believe that this is the case for this document, please contact UBIRA@lists.bham.ac.uk providing details and we will remove access to the work immediately and investigate.

Download date: 05. May. 2023

Accepted Manuscript

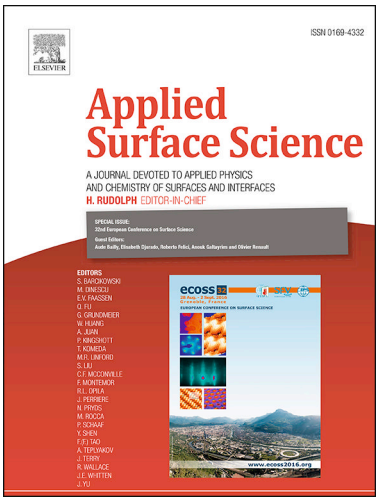


Full Length Article

# Effect of pulse frequency on the one-step preparation of superhydrophobic surface by pulse electrodeposition

Shuzhen Jiang, Zhongning Guo, Yu Deng, Hanshan Dong, Xiaoying Li, Jiangwen Liu

PII: S0169-4332(18)32014-2
DOI: https://doi.org/10.1016/j.apsusc.2018.07.120
Reference: APSUSC 39935

To appear in: *Applied Surface Science*

Received Date: 21 April 2018
Revised Date: 2 July 2018
Accepted Date: 17 July 2018

Please cite this article as: S. Jiang, Z. Guo, Y. Deng, H. Dong, X. Li, J. Liu, Effect of pulse frequency on the one-step preparation of superhydrophobic surface by pulse electrodeposition, *Applied Surface Science* (2018), doi: https://doi.org/10.1016/j.apsusc.2018.07.120

This is a PDF file of an unedited manuscript that has been accepted for publication. As a service to our customers we are providing this early version of the manuscript. The manuscript will undergo copyediting, typesetting, and review of the resulting proof before it is published in its final form. Please note that during the production process errors may be discovered which could affect the content, and all legal disclaimers that apply to the journal pertain.

ACCEPTED MANUSCRIPT

# Effect of pulse frequency on the one-step preparation of superhydrophobic surface by pulse electrodeposition

**Shuzhen Jiang [a], Zhongning Guo [a], Yu Deng [a], Hanshan Dong [b], Xiaoying Li [b] , Jiangwen Liu [a,*]**

[a] School of Electromechanical Engineering, Guangdong University of Technology, Guangzhou 510006, PR China

[b] School of Metallurgy and Materials, The University of Birmingham, Edgbaston, Birmingham, B15 2TT, UK

* Correspondence: gdutjwliu@gmail.com; Tel.: +86-20-3932-2412

**Abstract:** A union of surface with rough micro/nano structures and low surface free energy is critical for the preparation of superhydrophobic surfaces. In this study, a rapid one-step pulse electrodepositing method was used to prepare superhydrophobic surfaces on Cu substrates. The electrolyte was prepared with ethanol, myristic acid ($CH_3(CH_2)_{12}COOH$) and lanthanum chloride ($LaCl_3{\cdot}6H_2O$). The surface morphology, chemical composition and superhydrophobic property were characterized by SEM, XRD, FTIR, EDX, optical contact angle instrument and high-speed camera. It turned out that the deposited surfaces have micro/nano hierarchical structures mainly being composed of lanthanum myristate. It is found that the optimal water contact angle is approximately 160.3° with a sliding angle of around 5°. The effects of pulse frequency on the surface morphology and wettability were specifically studied and discussed under an equivalent electrolytic time of 10 min. In this way, it can effectively save time and be simply applied to other materials with good conductivity and has a promising wide range application.

**Keywords:** Superhydrophobicity; Wettability; Pulse-electrodeposition; Frequency

## 1. Introduction

Surfaces and interfaces are the keys to fulfill the functionality of devices and materials, and so the construction of surface micro/nano structures has great significance to the performance of materials[1, 2]. Wettability, one of the foremost features of a solid material, has been extensively researched in recent years. Usually, the static water contact angles (WCA) above 150° are identified as superhydrophobic surfaces, while indications about the adhesion of water droplets are given by the hysteresis and the sliding angle (SA)[3]. Such surfaces have attracted enormous research interest in light of their applications in self-cleaning, anti-icing, anti-corrosion, bactericidal surfaces, water-oil separation and so on[4-10]. The superhydrophobic phenomenon is due to a suitably roughened surface having a particular micro-nanostructures and/or material with low surface energy.

Enlighten by several kind of plants and insects in nature, such as rose petal[11], lotus leaf [12, 13], rice leaf[14], cicada wings[8] and mosquito complex eyes[15], numerous ways are sought to prepare surfaces of man-made superhydrophobicity, including electrochemical corrosion[16, 17], chemical corrosion[18-20], solution-immersion[21, 22], sol-gel processing[23, 24], femtosecond laser ablation[25, 26], CVD[27], electro-spinning[28], hybrid processes[29-32], etc. Nevertheless, there are a few disadvantages such as chemical pollution, ultra-clean and high vacuum operating conditions, high-priced equipment (e.g. photolithographic equipment), time-consuming, complicated multi-step machining with most of the methods mentioned above, which restrict their extensive potential applications.

Direct current (DC) electrodeposition[33-39] has aroused great interest among the research staff for the preparation of superhydrophobic surfaces on conductive materials due to its appealing advantages of low cost, facility and high efficiency. Furthermore, no matter how complicated the

ACCEPTED MANUSCRIPT

geometric shape of the substrates is, the feasibility of the mass production in industrial applications is an obvious superiority of cathodic electrodeposition. Besides, the surface morphology of the deposits is able to be easily controlled by changing the processing parameters such as electrical parameters, concentration and composition of electrolyte, machining time and temperature. Rare earth elements (REE) were applied to the preparation of superhydrophobic surfaces owing to its effective role in enhancing thermal stability as well as anti-corrosion of advanced functional materials[7]. Y. Liu et al., prepared cerium myristate superhydrophobic surface with controlled adhesion by electrodeposition[34]. T. Ishizaki et al., studied the corrosion resistance and durability of superhydrophobic surfaces formed on a magnesium alloy coated with a nanostructured cerium oxide film and fluoroalkylsilane molecules[40]. W.J. Xiao et al., tuned the wettability of $La_{0.7}Sr_{0.3}MnO_3$ coatings from superhydrophilicity to superhydrophobicity by hierarchical microstructure[41].

Compared with conventional DC electrodeposition in which only the potential or current can be adjusted, pulse electrodeposition can provide better control on the structure of electrodeposits as well as their performance by adjusting duty ratio and frequency. These unique parameters offer the opportunity to perturb the adsorption-desorption phenomenon at the cathode/electrolyte interface (catholyte), which has a considerable impact on the nucleation rate and the growth rate of crystals during the electro-crystallization, and ultimately decide the size and shape of crystals[42-44]. Different from the direct current deposition method, the pulse electrodeposition owns some unique advantages, such as rapid refreshment of adsorptive ions, thin diffusion layer, high deposition efficiency and convenient control of surface morphology. Apparently, the forming mechanisms of pulse electrodeposition are different from that of DC electrodeposition.

Nonetheless, to our knowledge, there are only a few explorations and reports on preparing superhydrophobic surfaces by pulse electrodeposition[38, 45-47]. Although, in these studies, a number of superiorities over the DC deposition method have been discussed, seldom systematic study has been conducted to investigate the influence of the electrical parameters of the pulsed current on the morphologies of the deposits as well as their effect on wetting properties.

Taking the above background into account, in this study, a one-step processing method for preparing of superhydrophobic surfaces was presented. The effect of pulse frequency on the surface structure and wettability of the deposits was studied by pulse electrodeposition with an electrolytic solution containing REE. According to the results of experiments, the forming mechanism of the deposited layer and performance of superhydrophobicity are discussed. With the advantages of simplicity, low toxicity, cost-effectiveness and greater control, this presented method could be simply applied to other conducting materials with a promising future for wide applications.

## 2. Materials and Methods

### *2.1. Materials and sample preparation*

Analytically pure myristic acid ($CH_3(CH_2)_{12}COOH$) and absolute ethanol were purchased from Damao Chemical Co., Ltd. Lanthanum chloride ($LaCl_3 \bullet 6H_2O$) was supplied by Kemiou Chemical Reagent Co., Ltd, which can be used without purifying. Copper plates were employed as the substrates for the preparation of deposited layers. Firstly, the copper substrates with the size of 30 mm × 30 mm × 1 mm, were ground with abrasive papers (grade 800 - 2000), afterward, degreased ultrasonically in absolute ethanol for 10 min, and then ultrasonically cleaned in deionized water for 10 minutes and finally dried at natural atmosphere.

### *2.2. Pulse electrodeposition*

To prepare electrolytes, 0.1 M $CH_3(CH_2)_{12}COOH$ and 0.04 M $LaCl_3 \cdot 6H_2O$ were solved with 150 ml absolute ethanol under magnetic agitation at room temperature. The anode and cathode were both copper plates and the distance between them was set by 2 cm in the beaker. With voltage of 30 V and a duty ratio of 50%, pulse currents with frequencies ranging from 5 to 3000 Hz were applied by using

ACCEPTED MANUSCRIPT

a pulse power supply (ELGAR SW5250A, USA). Table 1 shows the electrical parameters and the composition of the electrolyte. The waveforms of the pulse current applied in the experiments are exemplified in Fig. 1. The used solution was replaced with fresh electrolyte to avoid pollution and lower the effects of solution concentration after each sample was prepared. All the samples were treated with an equivalent electrolysis time for 10 minutes at ambient temperature under agitation condition by a magnetic agitation setup with a rotation rate of 200 rpm. After that, ethanol and distilled water were used to wash the cathode for several times under atmospheric condition. Ultimately, the superhydrophobic surfaces with hierarchical micro-nanostructures were prepared.

**Table 1.** Experimental parameters of the pulse electrodeposition

| Current parameters | value | Electrolyte parameters | value |
|---|---|---|---|
| Voltage(V) | 30 | Lanthanum chloride (M) | 0.04 |
| Duty ratio | 50% | Myristic acid (M) | 0.1 |
| Frequency(Hz) | 5,50,500,1k,2k,3k | Ethanol (ml) | 150 |

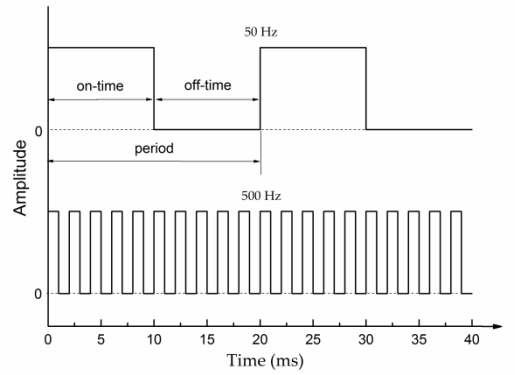


**Fig. 1.** An example of pulse waveforms

*2.3. Sample characterization*

The surface morphologies and the corresponding surface elements of the deposits were investigated by a scanning electron microscope (SEM, JEOL JSM 6060LV, Japan) equipped with an energy dispersive spectrometer (EDX, Genesis 60, USA). To investigate the cross-sectional structure of the deposited layer, a focused ion beam field emission scanning electron microscope (FIB-FESEM, LYRA 3 XMU, Tescan, Czech) was operated at 5kV to observe the surface and its FIB module was used to accurately remove materials from the as-prepared surface and then the SEM was used to observe the fabricated cross-section. The 3D profile and the corresponding surface roughness were measured by a white light interferometer (Bruker Contour GT-X, Germany). The average of six measurements at different locations on the samples was reported. The details of functional group were probed by an Fourier transform infrared spectrophotometer (FTIR, NICOLET 8700, USA) while the crystalline details was examined by an X-ray diffractometer (Bruker D8, Germany) applied with 40 kV and 40 mA and monochromatic Cu K$\alpha$ radiation ($\lambda$=0.15418 nm). Water contact angles were measured by an optical contact angle meter (XG-CAMB1, China) under room temperature for each sample. By vibrating the burette, about 4μl water droplets were fallen onto the deposition layers from a height of 20 mm. The sliding angles were measured and read from an angle scale which installed on the tilting platform. Five measurements were detected at different locations on the same sample to

ACCEPTED MANUSCRIPT

obtain the average. The water bouncing was photographed with 400 fps by a high-speed photography system (Fastec HiSpec5, USA).

## 3. Results

### *3.1. Surface morphology*

Morphology is one of the decisive factors of the wettability of surfaces. Fig. 2 demonstrates the SEM images of the deposited surfaces obtained for various frequencies under 30 V and 50% duty ratio after an equivalent electrolysis time of 10 minutes. Fig. 2a shows the morphology of the as-prepared surface deposited under 5 Hz condition. As demonstrated in Fig. 2a, urchin-like clusters with a diameter of about 300 μm were formed on the comparatively well-distributed micro particles which have a diameter of around 15-30 μm. The inset image in Fig. 2a reveals that the thorns of the urchin-like structures are sharp and have a length of about 150 μm. When the frequency was increased to 50 Hz, the urchin-like clusters disappeared and the flower-like clusters substituted (Fig. 2b). With a diameter of around 50-80 μm, these clusters have countless and compact overlapping petals, which makes it similar to blooming flowers. Beneath the flower-like clusters, particles with a diameter of about 5-15 μm were deposited relatively uniformly. An enlarged image of partial (Inset of Fig. 2b) showed that the petals are actually formed with rope-like structures and with a diameter of about 1μm. When the frequency was further increased to 500 Hz, the SEM image of the surface morphology is shown in Fig. 2c. The flower-like clusters can also be found on the deposited surface. However, the petals of the flower-like clusters are looser than the ones shown in Fig. 2b. Around and under the flower-like clusters, particles with a diameter of about 5-15 μm were deposited which lead to heterogeneous surface structures.

In order to provide more details of the flower-like clusters, a focused ion beam was used to fabricate a cross-section of the deposited layer obtained under 50 Hz. As shown in Fig. 3a, the flower-like cluster, with a diameter of about 80 μm, was semispherical and deposited on the small size particles. The petals of the flower-like structure were radial. After the fabrication using the focused ion beam, the cross-sectional image of the flower-like structure was shown in Fig. 3b. The stripe pattern of the cross-section was the fabricated trace caused by FIB, which is so called “stream effect”. According to the cross-sectional image, the inner part of the flower-like structure was solid, with a diameter of about 50 μm. Many rope-like structures were evolved and grown radically on the spherical solid core, with a length of about 15 μm, and finally formed into the flower-like cluster.

Fig. 2d shows the surface morphology of the pulsed electrodeposition under a high frequency of 1000 Hz. Under this condition, neither the urchin-like clusters nor the flower-like clusters could be found on the deposited surface. Only the relatively uniform mastoids with a diameter of around 5-15 μm were agglomerated. In addition, the interconnected hair-like nanostructure of about 1 μm in length and 50 nm in width could be found on the micro-scale convex structures. As shown by the inset of Fig. 2d, the high magnification image revealed the integration of micro/nano hierarchical structures, which is similar to the surface structure of lotus leaves. Therefore, the deposited layer acquired under such conditions presented a highly textured surface. With the increasing of frequency from 2000 to 3000 Hz, the images of SEM are shown in Fig. 2e and 2f. It is clear that the surfaces obtained under such conditions have similar morphology. Almost all particles of about 5-15 μm in diameter have cracks on the surface, which made them similar to the shape of coffee beans. The inset of Fig. 2f reveals that these micro particles have nano-scale roughness which enhances their heterogeneous texture.

ACCEPTED MANUSCRIPT

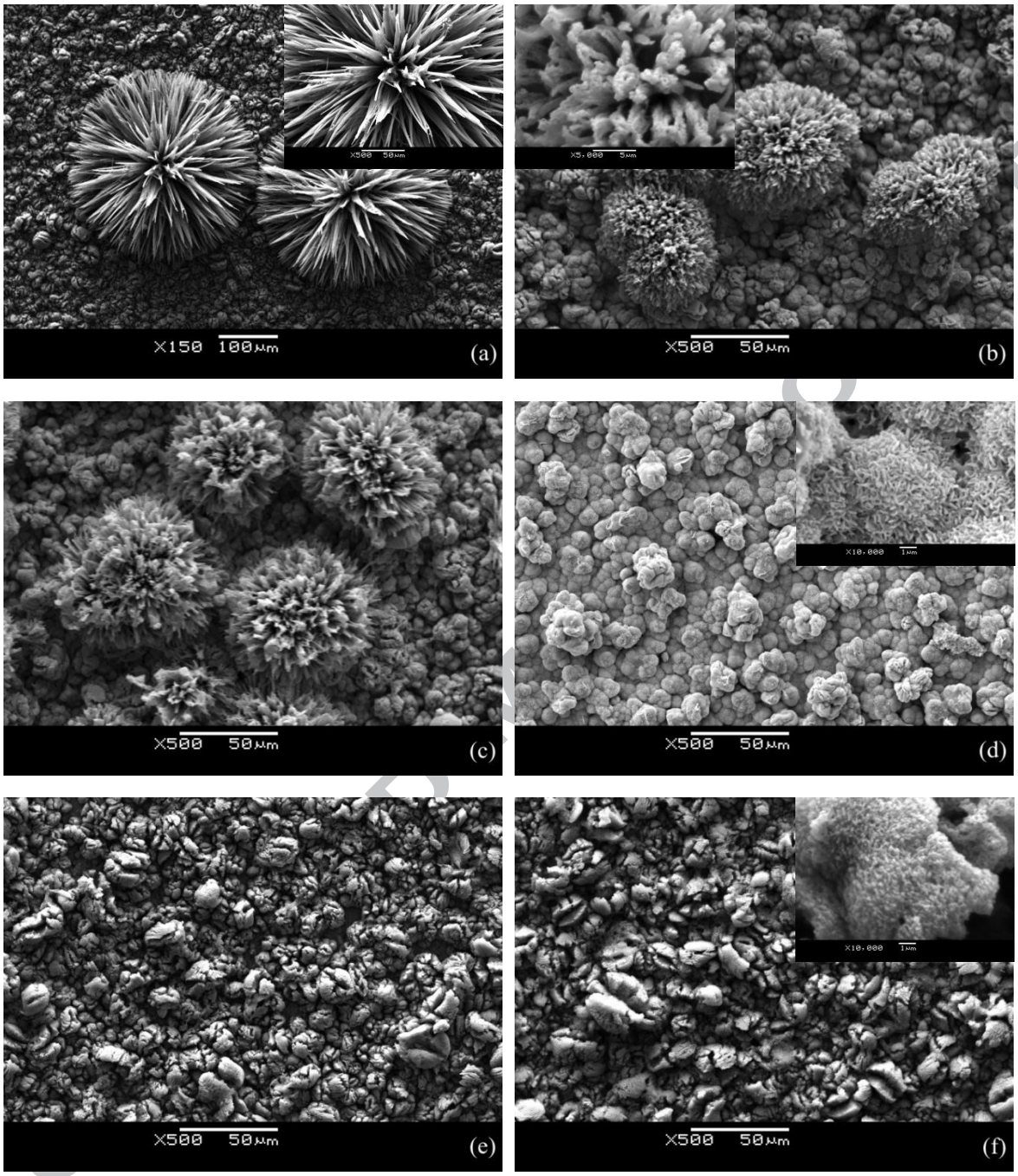


**Fig. 2.** SEM images of the deposited surfaces with various frequencies at 30V and 50% duty ratio pulse current.(a) 5 Hz; (b) 50 Hz; (c) 500 Hz; (d) 1000 Hz; (e) 2000 Hz; (f) 3000 Hz.

ACCEPTED MANUSCRIPT

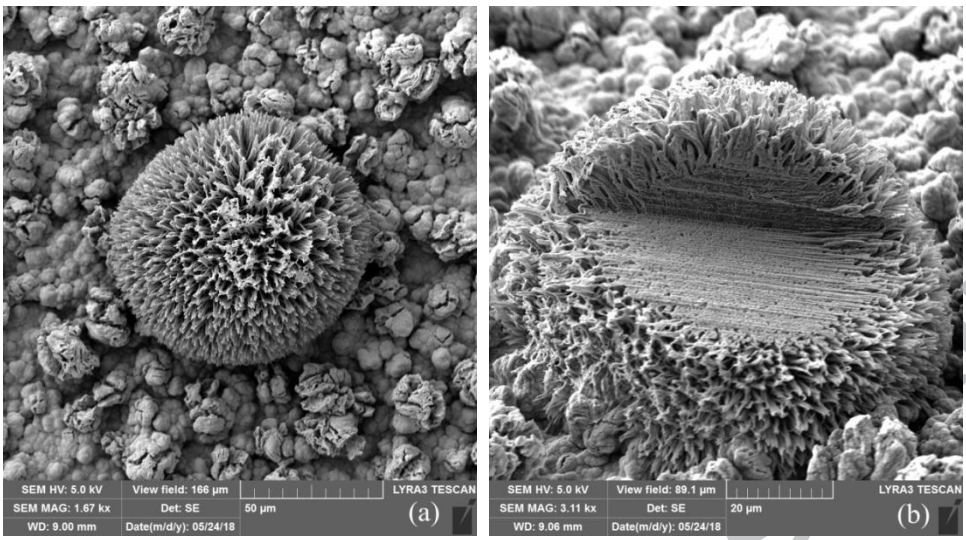


**Fig. 3.** SEM images of the sample surface obtained under 30V, 50Hz and 50% duty ratio(a) and its cross-section after the fabrication by focus ion beam(b).

To investigate the relationship between the pulse frequencies and the surface roughness, a white light interferometer was used to characterize the 2D and 3D surface roughness, with a sampling area of 620×465 μm. Figs. 4a-b showed the contour images of the as-prepared surface obtained under 5Hz. The distribution of the colours revealed that the surface consisted of large size cluster of about 250μm in diameter and many small size rough structures around the large cluster, which is in accordance with the urchin-like structure observed in Fig. 2a. Figs. 4c-d showed the contour images of the as-prepared surface obtained under 1000Hz. As revealed by the distribution of the colours and values, the surface obtained under such condition had no large clusters with only particles of about 15μm in diameter distrusted relatively evenly on the surface. Moreover, these particles were overlapping each other, which is in line with the result shown in Fig. 2d.

As shown in Fig. 5, the Ra of bare coppers after polishing is only about 0.25 μm while the Ra of the as-prepared surfaces coated under 5, 50, 500, 1000, 2000 and 3000 Hz is 5.09, 4.41, 4.37, 3.05, 3.94 and 4.03 μm, respectively. Clearly, the Ra value firstly decreased with the frequencies and then slightly increased.

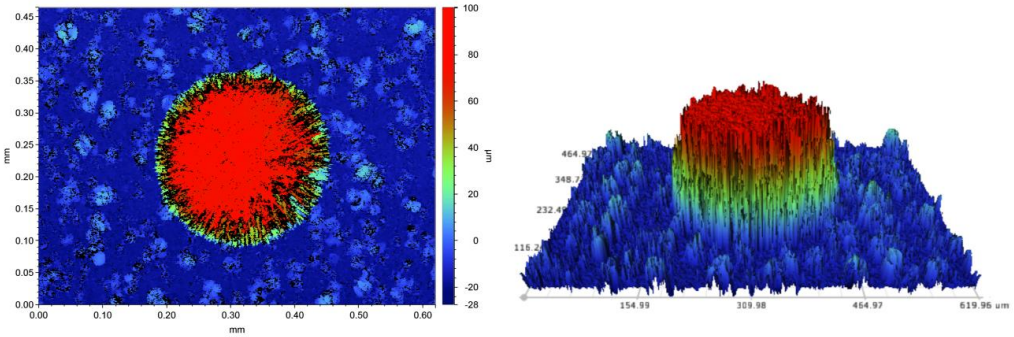


(a) (b)

ACCEPTED MANUSCRIPT

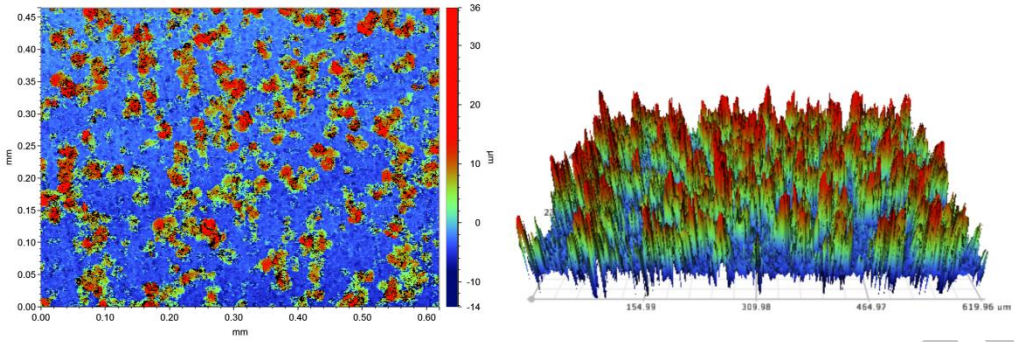


(c) (d)

**Fig. 4.** 2D and 3D contour images of the deposited surfaces with various frequencies at 30V and 50% duty ratio pulse current.(a)(b) 5 Hz; (c)(d) 1000 Hz;

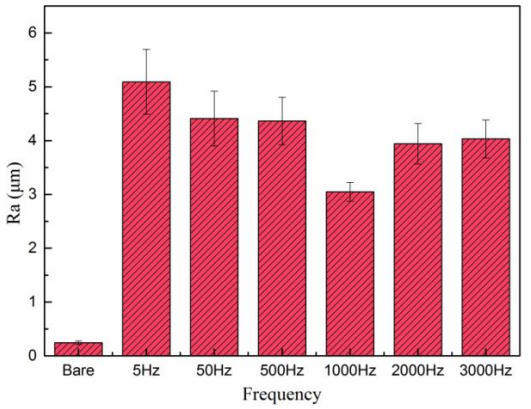


**Fig. 5.** The surface roughness of the polished copper plate and the as-coated surfaces deposited at 30V and 50% duty cycle pulse current for different frequencies.

*3.2. Phase and Chemical composition*

The crystalline information and chemical composition of the as-prepared surfaces were analyzed by employing XRD, FTIR, and EDX spectra. As shown in Fig. 6, the phase information of the superhydrophobic surface acquired under the application of pulse current with 30 V, 1000 Hz and 50% duty ratio was given by the XRD pattern recorded with a 2θ range of 1.5~20.0°. Within the small angle range from 4.5° to 12.0°, a group of well-defined diffraction peaks labeled with ($l_n$,0,0) could be found, which implied that the deposited layer is crystallized and has a layer structure [48, 49] although the mechenisim involved is still under investigation.

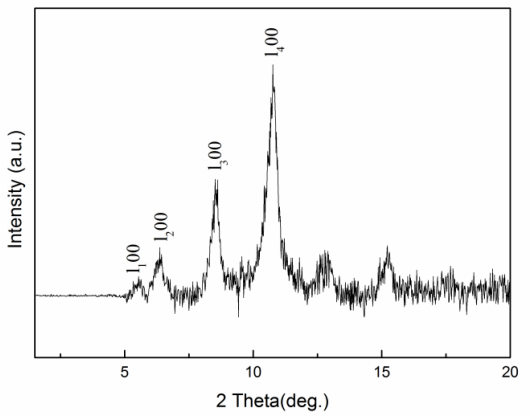

ACCEPTED MANUSCRIPT

**Fig. 6.** XRD spectrum of the superhydrophobic surface prepared under 1000 Hz

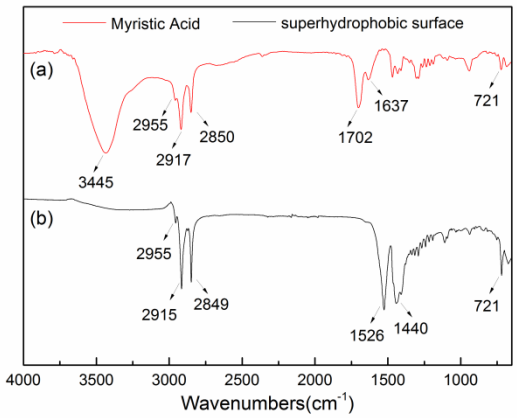


**Fig. 7.** FTIR spectra of (a) pure myristic acid and (b) the superhydrophobic surface obtained under 1000 Hz

As shown in Fig. 7, the FTIR spectra were applied to obtain the functional group details of the pure myristic acid and the deposited layer prepared at 1000 Hz. On one hand, the absorption peak corresponding to the free carboxyl group (-COO-) from pure myristic acid could be found at 1702 $cm^{-1}$ when the frequency was lower while the deposited layer showed the adsorption peaks at 1440 $cm^{-1}$ and 1526 $cm^{-1}$. This might be caused by the asymmetric and symmetric stretching of carboxyl group result from its carboxylate form with a metal atom. On the other hand, when the frequency was higher, the absorption peaks at 2915 $cm^{-1}$ and 2849 $cm^{-1}$ are attributed to methyl groups (-$CH_2$-) symmetric and asymmetric stretching vibrations and the absorption peaks at 2955$cm^{-1}$ are ascribed to methylene groups (-$CH_3$) asymmetric stretching vibrations. The plane wave absorption peak appeared at 721 $cm^{-1}$ belongs to the characteristic absorption peak of -$CH_2$- if four or more -$CH_2$- exist in the carbon chain. According to scientific report, the surface free energy of -$CH_3$ and -$CH_2$- groups are 24 $mJ/m^2$ and 31 $mJ/m^2$, respectively[50], indicating that the surface free energy of the deposited layers are relatively low. Furthermore, a very prominent broad peak found around 3445 $cm^{-1}$ and a strong absorption peak at 1637 $cm^{-1}$ in Fig. 7a are attributed to hydroxyl groups (-OH) stretching vibration and in-plane bending vibration respectively, which disappears in Fig. 7b, supports the formation of metal myristate[51]. Thus, the water-repellent long alkyl chains (namely, $C_{13}H_{27}COO^-$) have been successfully deposited onto the surface of copper substrate.

An EDX spectrum of the superhydrophobic surface deposited at 1000 Hz is depicted in Fig. 8. There are mainly four elements, La, C, O and Cl. The atomic percentage of La/C/O was listed in Table 2, which was about 1:35.07:5.18. It is similar to the La/C/O atomic ratio (1/42/6) in lanthanum myristate ($La[CH_3(CH_2)_{12}COO]_3$). This measured atomic ratio is acceptable if taking the measurement errors of light elements (C & O) from heterogeneous morphology into consideration. Therefore, according to the chemical valences of $La^{3+}$ and $CH_3(CH_2)_{12}COO^-$ in the electrolyte and the La/C/O atomic ratio of the as-prepared sample, it can be deduced that the deposited layer on the copper substrates mainly contains $La[CH_3(CH_2)_{12}COO]_3$. As long chain aliphatic acid having hydrophobic hydrocarbon side effects[19], lanthanum myristate has low surface free energy.

ACCEPTED MANUSCRIPT

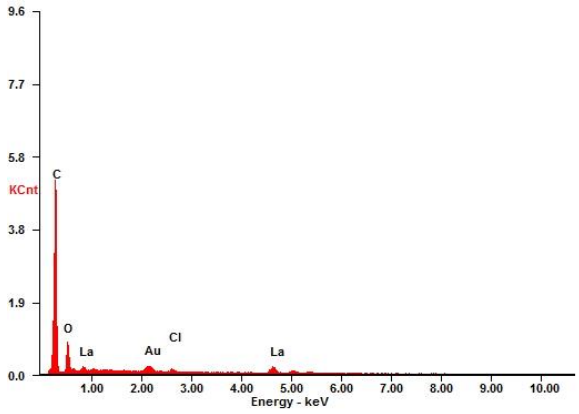


**Fig. 8.** EDX spectrum of the pulse-electrodeposited layer acquired at 1000 Hz

**Table 2.** Element data of the pulse-electrodeposited layer acquired by EDX Spectrum.

| Element | Weight % | Atom % |
|---|---|---|
| C-K | 64.63 | 84.52 |
| O-K | 12.73 | 12.49 |
| Cl-K | 1.31 | 0.58 |
| La-L | 21.33 | 2.41 |
| Total | 100 | 100 |

*3.3. Surface wettability*

As shown in Fig. 9, the contact angles and sliding angles of the deposited layers were measured, which revealed the correlation between the hydrophobicity of the deposited surfaces and the frequency of the pulse current. After modified with pure myristic acid, the WCA of the polished copper plate is about 107.5° [41]. The WCA of the deposited layer increased to 150.4° with a SA of approximately 12° when applied with a current of 30 V, 50% duty ratio and 5 Hz, which indicated that the wettability has already reached the superhydrophobic state. When the frequency increased to 50 Hz, the WCA was raised to 155.5° while a SA reduced to 8°, which indicated that the surface had low adhesion. However, the WCA slightly decreased to 153.6° while the SA remained almost the same at 8° when the frequency increased to 500 Hz. The WCA was raised to 160.3° with a SA further decreased to about 5° as the frequency increased to 1000 Hz. However, the WCAs were slightly decreased to 157.0° and 156.7° and the corresponding SA slightly increased to 6° with the increasing of frequency to 2000 and 3000 Hz respectively, but still met the superhydrophobic standards.

ACCEPTED MANUSCRIPT

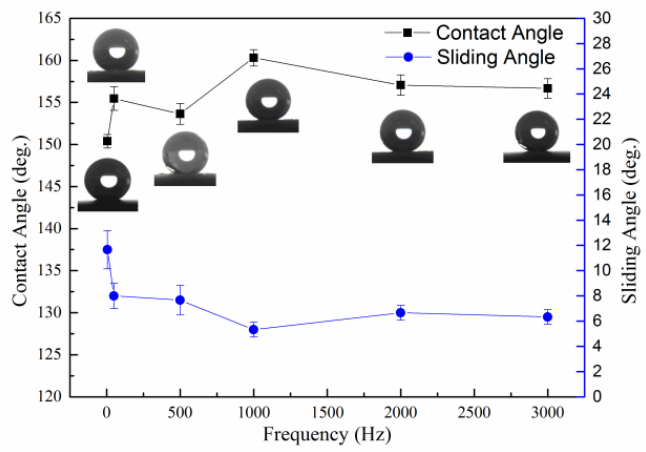


**Fig. 9.** Correlation between the water contact angle & sliding angle and the pulse current frequency.

If a surface has a property of water repellency, droplets would jump up rather than wet the surface [52]. In order to study the effect of micro/nano hierarchical structure on the durability of the superhydrophobic layer, a high-speed camera was applied to seize the droplet motion before and after it hit the pulse-electrodeposited layer which prepared at 1000 Hz condition and exposed in the atmosphere for ten months. From a height of 4 cm, a water droplet freely fell and collided the superhydrophobic surface and totally bounce back. The impact velocity is approximately 88.5 $cm \cdot s^{-1}$. As shown in Fig. 10, obviously, there was no residual droplet left on the surface of the cathode, which indicated that the droplet totally bounced away from the surface. However, because of slightly increasing of adhesion, the droplet almost spitted into two at 18.75ms, which indicated that the status of wettability has slightly changed after a long time of exposure in the air. In spite of this phenomenon the superhydrophobic layer still maintained outstanding nonsticking characteristics. Obviously, the deposited surface had a long-term stability of superhydrophobicity and resemble to the lotus effect which has remarkable self-cleaning characteristics.

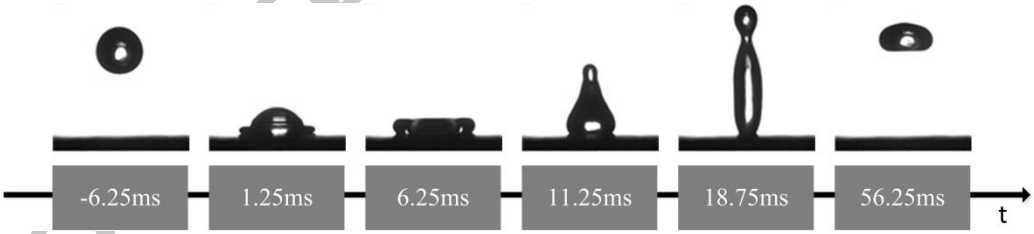


**Fig. 10.** Bouncing phenomenon of the water droplet on the as-obtained surface at 1000 Hz

## 4. Discussion

### *4.1. Effect of current frequency on surface morphologies*

Electrocrystallization consists of three basic steps: seed generation, nucleation and crystal growth. Firstly, seed crystals appear on the cathode/electrolyte interface (catholyte). Afterward, the seed crystals grow continuously and evolve into crystal nuclei when reaching the critical size. Ultimately, the nuclei grow into crystals. During the electrocrystallization process, the crystal nucleation rate and growth rate have a close relation to the grain size and density.

In this research, the duty ratio of the current is 50%, which means that the on-time and off-time of the current are equal. The frequency determines the length of the period as well as the on-time and off-time of the current. During the current on-time, the $La^{3+}$ close to the cathodic electrode react with $CH_3(CH_2)_{12}COOH$ resulting in the forming of $La[CH_3(CH_2)_{12}COO]_3$, meanwhile some $H^+$ ions are generated on the cathode. The free $H^+$ ions capture the free electrons generated from the anodic

ACCEPTED MANUSCRIPT

electrode and were evolved into $H_2$, forming bubbles surrounded the cathode. Base on the electrochemical theory, reactive chemicals and the chemical composition data acquired by EDX and XRD, the reaction equations could be concluded by the following Equations (1) and (2).

$$La^{3+} + 3CH_3(CH_2)_{12}COOH \rightarrow La[CH_3(CH_2)_{12}COO]_3 + 3H^+ \quad (1)$$

$$2H^+ + 2e^- \rightarrow H_2 \uparrow \quad (2)$$

The evolution of $H_2$ gases agitates the electrolytic solution, promoting the forming of the highly textured structure on the cathode. In addition, no Cu element appears on the EDX spectrum which means that there is no codeposition of Cu ions. The reason may be that the concentration of dissolved Cu ions is much lower than the hydrogen ions. This could be mainly ascribed to the formation of $CuCl_2$ passivation film on anodic surface.

However, in the intervals of the pulse current, a large amount of positive ions moves towards the cathode, promoting the sufficient recovery of the positive ion concentration of the dilute vicinity of cathode. At the same time, the intervals of pulse current also suppress the epitaxial growth and thus prevents the further crystal growth.

Furthermore, the frequency of the pulse current would affect the nucleation rate of grains by[46]:

$$J = K\exp(-\frac{\pi\sigma_1^2 M}{\rho nFRT}\frac{1}{\eta}) \quad (3)$$

Where $J$ is the nucleation rate, $K$ is relative to the energy for the nucleation, $\sigma_1$ is the surface free energy between the solution and the grain, $M$ is the atomic weight, $\rho$ is the density of the deposited layer, $n$ is the number of electrons, $F$ is the Faraday constant, $R$ is the gas constant, $T$ is the time of 1 pulse cycle, and $\eta$ is the over-potential. Obviously, when applying with high pulse frequencies, the nucleation rate $J$ is enhanced, leading to retardation of the crystal growth.

According to the discussion above, the frequency affects the mechanism of electrocrystallization by affecting the nucleation rate and the growth rate of crystals. Obviously, the frequency is a critical factor for deciding the morphologies and thus the superhydrophobicity. For instance, when the current frequency was only 5 Hz, the on-time and the off-time was 200 ms, the consumption of reactants in the vicinity of the cathode was so quick and the electrolyte concentration near cathode reduced correspondently, leading to the domination of mass transfer other than electrochemical reaction. Hence, competitive crystal growth became more prominent than nucleation, leading to the formation of urchin-like microstructures. When the frequency increased to 50 and 500 Hz, the pulse width decreased and the proportion of crystal growth correspondingly weaken. The micro crystals formed at such conditions had flower-like structures as shown in Fig. 2b and 2c. In fact, when the frequency is too low, the pulse electrodeposition will lose the superiority of rapid refreshment of adsorptive ions and possession of a thin diffusion layer, thereby approaching the effect of DC electrodeposition.

Further increasing the frequency to 1000 Hz resulted in the disappearance of large clusters and only relatively well-distributed particles occurred. It was interesting to notice that hair-like nanostructures were overlaid on the microstructures. It may be due to the fact that nucleation rate and growth rate play a relatively equal role under such condition. Although the involved mechanism still need to be studied, this hierarchical micro/nano structure is resemble to the structure of lotus leaves and might be a great contribution to the highest WCAs about 160.3°. With the increasing frequency to 2000 and 3000 Hz, the on-time were only 0.25 and 0.17 ms and the competitive nucleation rate became more pronounced than crystal growth, thus resulting in smaller size of particles than the other surfaces prepared by a lower frequency.

*4.2. The wettability of the pulse electrodeposited surfaces*

ACCEPTED MANUSCRIPT

As shown in the previous section, Fig. 2 reveals that the morphologies of the as-obtained surfaces have a close correlation with the pulse current frequency. Compared with an untreated copper plate, all the deposited surfaces demonstrated remarkably increased WCA to the superhydrophobic state. This might be ascribed to the formation of $La[CH_3(CH_2)_{12}COO]_3$ by electrocrystallization with low surface free energy (Figs. 6, 7 & 8) combined with hierarchical micro/nano structures (Fig. 2).

The frequency of pulse current ranged from 5, 50 to 500 Hz, the WCA of the deposited surfaces were 150.4°, 155.5° and 153.6° with a SA of 12°, 8°, and 8° respectively. All of the surfaces prepared under these conditions presented the similar property: formation of relatively large clusters larger than 50 μm which deposited on the relatively uniform micro particles with a diameter of about 5-15 μm. The surface with the urchin-like structure obtained under 5 Hz demonstrated the poorest superhydrophobicity while the surface with the tight flower-like structure obtained under 50 Hz showed a slightly better hydrophobicity than the surface with the loose flower-like structure obtained under 500 Hz. It can be presumed that the water droplets easily tend to penetrate into the gaps of such large and loose clusters and get stuck than the small and tight ones, leading to the difference of wetting performance.

With further increase of frequency to 1000 Hz, the urchin-like or flower-like structures disappeared and the obtained surface exhibited the highest WCA (160.3°) with lowest SA (5°). When the frequency was further increased to 2000 and 3000 Hz, the WCA slightly reduced (157.0° and 156.7°) rather than increased, although both the surfaces had a similar micro particle size with the one prepared under 1000 Hz. Obviously, this phenomenon cannot be simply elucidated from the perspective of particle size and surface energy and there should be other potential mechanisms need to be revealed.

Close characterization of the morphology of electrodeposited layers prepared at 1000, 2000 and 3000 Hz has shown hierarchical micro/nano structures. As revealed in Fig. 2d, the overlapping hairy-like nanostructures are superimposed on the top of the microstructures. This kind of surface morphology is resembled to the properties of lotus leaves and might be the reasonable explanation for the measured wettability with the highest WCA approximately 160.3° and the lowest SA approximately 5°. Nevertheless, the nanostructures formed on the superhydrophobic surfaces prepared at 2000 and 3000 Hz (Fig. 2e & 2f) are not so distinctly developed as the one prepared at 1000 Hz (Fig. 2d).

Combined with low surface energy, the construction of rough structures on the surface has led to the significant improvement of water repellency compared with polished substrate. As shown in Fig. 5, the Ra value of the deposited surfaces firstly decreases with the frequencies and then slightly increases; however, the highest WCA (160.3°) was obtained under the surface with the lowest Ra value (3.05 μm). This indicates that the surface roughness should have an optimal value other than simply consider that rougher surfaces will achieve better hydrophobicity.

It is generally accepted that if the sliding angle is less than 10°, the superhydrophobic surface is in a Cassie-Baxter state. According to the observation above, the superhydrophobicity of the pulse electrodeposited surface prepared under 1000 Hz could be expressed by Cassie–Baxter equation[53]:

$$\cos\theta_r = f_1 \cos\theta - f_2 \tag{4}$$

where $f_1$ is the area fraction of solid surface and $f_2$ is that of the air, moreover, $f_1 + f_2 = 1$; $\theta_r$ is the apparent CA of the roughened surface while $\theta$ is the intrinsic CA of the flat surface. For this research, the WCA of the polished Cu plates modified with $CH_3(CH_2)_{12}COOH$ is only about 107.5° while the deposited layer with highly textured surface is about 160.3°. Therefore, the value of $f_1$ and $f_2$ could be figured out as 0.0837 and 0.9163 separately, which indicated that only 8.37% droplet bottom is supported by the deposits directly while about 91.63% droplet bottom is in touch with the air of the gaps. The interface between the water and the air was increased by the trapped air, thereby stopping the wetting of water on the surface. The highly textured surface allows droplets to be

ACCEPTED MANUSCRIPT

supported by the air cushion, leading to a significant increase of WCA. This obviously showed that the air cushion is a critical reason for improving the superhydrophobic performance of the surface and it is the formation of hierarchical micro-nanostructure during the electrocrystallization with an optimal current frequency that makes a contribution to the special superhydrophobic performance observed.

In short, the performance of the as-obtained surfaces and the applied frequencies during pulse eletrodeposition have a close correlation. The frequencies have a significant influence on the mechanism of electrodeposit formation by affecting the nucleation rate and the growth rate of crystals and ultimately affected the wettability.

## 5.Conclusion

Pulse electrodeposition has been successfully employed as a one-step processing method to achieve the preparation of superhydrophobic surfaces. An electrolyte consisting of ethanol, myristic acid and lanthanum chloride is adopted. As the experimental results revealed, the main conclusions could be drawn as follows.

- The pulse current frequency is a prominent factor which affects the formation mechanism of deposits and hence the surface morphologies.
- The electrodeposited layer mainly contains lanthanum myristate, which possesses a union of hierarchical micro/nano structure and low surface free energy, has a great contribution to the superhydrophobic surface with a WCA of 160.3° and a corresponding SA of approximately 5°.
- After ten months exposure in the air since the deposition, the outstanding durability of the electrodeposited layers has been proved by the bouncing of the water droplet.
- This processing method is expected to be conveniently applied to some other potential materials with good conductivity for the preparation of advanced surfaces with superhydrophobic characteristics.

**Acknowledgements:** This work was supported by National Natural Science Foundation of China (51575113, 51675105), the Department of Science and Technology of Foshan Municipality (2015IT100162), the Special Support Plan of the Guangdong province (2014TQ01X542) and the Fundamental Research Funds for the Central Universities (2015ZZ080). The authors also thank China Scholarship Council (State Scholarship Fund 201503780046) and British Council (Newton Fund: Ph.D. Placement grant) for providing scholarships for Shuzhen Jiang to enable him to conduct research work at University of Birmingham. Shuzhen Jiang would like to thank Hanshan Dong for the supervision of research and provision of research facilities in Birmingham UK.

## References

[1] T. Sun, L. Feng, X. Gao, L. Jiang, Bioinspired surfaces with special wettability, Accounts of chemical research, 38 (2005) 644-652.

[2] Y. Xia, J.A. Rogers, K.E. Paul, G.M. Whitesides, Unconventional methods for fabricating and patterning nanostructures, Chemical reviews, 99 (1999) 1823-1848.

[3] T. Darmanin, E.T. de Givenchy, S. Amigoni, F. Guittard, Superhydrophobic surfaces by electrochemical processes, Advanced materials, 25 (2013) 1378-1394.

[4] H. Bagheri, M. Aliofkhazraei, H.M. Forooshani, A.S. Rouhaghdam, Facile fabrication of uniform hierarchical structured (UHS) nanocomposite surface with high water repellency and self-cleaning properties, Applied Surface Science, 436 (2018) 1134-1146.

[5] M.A. González Lazo, I. Katrantzis, S. Dalle Vacche, F. Karasu, Y. Leterrier, A Facile in Situ and UV Printing Process for Bioinspired Self-Cleaning Surfaces, Materials, 9 (2016) 738.

[6] J.H. Li, Q. Liu, Y.L. Wang, R.R. Chen, K. Takahashi, R.M. Li, L.H. Liu, J. Wang, Formation of a Corrosion-Resistant and Anti-Icing Superhydrophobic Surface on Magnesium Alloy via a Single-Step Method, Journal of the Electrochemical Society, 163 (2016) C213-C220.

ACCEPTED MANUSCRIPT

[7] Y. Liu, S. Li, J. Zhang, J. Liu, Z. Han, L. Ren, Corrosion inhibition of biomimetic super-hydrophobic electrodeposition coatings on copper substrate, Corrosion Science, 94 (2015) 190-196.

[8] E.P. Ivanova, J. Hasan, H.K. Webb, V.K. Truong, G.S. Watson, J.A. Watson, V.A. Baulin, S. Pogodin, J.Y. Wang, M.J. Tobin, Natural bactericidal surfaces: mechanical rupture of Pseudomonas aeruginosa cells by cicada wings, Small, 8 (2012) 2489-2494.

[9] T.E. O'Loughlin, S. Martens, S.R. Ren, P. McKay, S. Banerjee, Orthogonal Wettability of Hierarchically Textured Metal Meshes as a Means of Separating Water/Oil Emulsions Advanced Engineering Materials, 19 (2017) 1600808.

[10] H. Bagheri, M. Aliofkhazraei, H.M. Forooshani, A.S. Rouhaghdam, Electrodeposition of the hierarchical dual structured (HDS) nanocrystalline Ni surface with high water repellency and self-cleaning properties, Journal of the Taiwan Institute of Chemical Engineers, 80 (2017).

[11] L. Feng, Y. Zhang, J. Xi, Y. Zhu, N. Wang, F. Xia, L. Jiang, Petal effect: a superhydrophobic state with high adhesive force, Langmuir : the ACS journal of surfaces and colloids, 24 (2008) 4114-4119.

[12] W. Barthlott, C. Neinhuis, Purity of the sacred lotus, or escape from contamination in biological surfaces, Planta, 202 (1997) 1-8.

[13] L. Feng, S. Li, Y. Li, H. Li, L. Zhang, J. Zhai, Y. Song, B. Liu, L. Jiang, D. Zhu, Super-hydrophobic surfaces: from natural to artificial, Advanced materials, 14 (2002) 1857-1860.

[14] J. Yao, J. Wang, Y. Yu, H. Yang, Y. Xu, Biomimetic fabrication and characterization of an artificial rice leaf surface with anisotropic wetting, Chinese Science Bulletin, 57 (2012) 2631-2634.

[15] C. Wu, X. Kong, D. Wu, Micronanostructures of the scales on a mosquito's legs and their role in weight support, Physical review E, 76 (2007) 017301.

[16] D.-D. La, T.A. Nguyen, S. Lee, J.W. Kim, Y.S. Kim, A stable superhydrophobic and superoleophilic Cu mesh based on copper hydroxide nanoneedle arrays, Applied Surface Science, 257 (2011) 5705-5710.

[17] J.-l. Song, W.-j. Xu, X. Liu, Y. Lu, J. Sun, Electrochemical machining of super-hydrophobic Al surfaces and effect of processing parameters on wettability, Applied Physics A, 108 (2012) 559-568.

[18] N. Saleema, D.K. Sarkar, D. Gallant, R.W. Paynter, X. Chen, Chemical Nature of Superhydrophobic Aluminium Alloy Surfaces Produced via a One-Step Process Using Fluoroalkyl-Silane in a Base Medium, ACS applied materials & interfaces, 3 (2011) 4775-4781.

[19] J. Yang, Z. Zhang, X. Xu, X. Men, X. Zhu, X. Zhou, Superoleophobic textured aluminum surfaces, New Journal of Chemistry, 35 (2011) 2422-2426.

[20] Y. Wang, W. Wang, L. Zhong, J. Wang, Q. Jiang, X. Guo, Super-hydrophobic surface on pure magnesium substrate by wet chemical method, Applied Surface Science, 256 (2010) 3837-3840.

[21] L. Zhao, Q. Liu, R. Gao, J. Wang, W. Yang, L. Liu, One-step method for the fabrication of superhydrophobic surface on magnesium alloy and its corrosion protection, antifouling performance, Corrosion Science, 80 (2014) 177-183.

[22] J. Song, Y. Lu, S. Huang, X. Liu, L. Wu, W. Xu, A simple immersion approach for fabricating superhydrophobic Mg alloy surfaces, Applied Surface Science, 266 (2013) 445-450.

[23] R. Lakshmi, T. Bharathidasan, B.J. Basu, Superhydrophobic sol–gel nanocomposite coatings with enhanced hardness, Applied Surface Science, 257 (2011) 10421-10426.

[24] L. Feng, H. Li, Y. Song, Y. Wang, Formation process of a strong water-repellent alumina surface by the sol–gel method, Applied Surface Science, 256 (2010) 3191-3196.

[25] B. Wang, X. Wang, H. Zheng, Y.C. Lam, Surface Wettability Modification of Cyclic Olefin Polymer by Direct Femtosecond Laser Irradiation, Nanomaterials, 5 (2015) 1442-1453.

[26] E. Fadeeva, V.K. Truong, M. Stiesch, B.N. Chichkov, R.J. Crawford, J. Wang, E.P. Ivanova, Bacterial retention

ACCEPTED MANUSCRIPT

on superhydrophobic titanium surfaces fabricated by femtosecond laser ablation, Langmuir : the ACS journal of surfaces and colloids, 27 (2011) 3012-3019.

[27] T. Ishizaki, J. Hieda, N. Saito, N. Saito, O. Takai, Corrosion resistance and chemical stability of super-hydrophobic film deposited on magnesium alloy AZ31 by microwave plasma-enhanced chemical vapor deposition, Electrochimica Acta, 55 (2010) 7094-7101.

[28] J. Yang, C. Liu, B. Wang, X. Ding, Feedback System Control Optimized Electrospinning for Fabrication of an Excellent Superhydrophobic Surface, Nanomaterials, 7 (2017).

[29] Y. Lu, S. Sathasivam, J. Song, C.R. Crick, C.J. Carmalt, I.P. Parkin, Robust self-cleaning surfaces that function when exposed to either air or oil, Science, 347 (2015) 1132-1135.

[30] Q.X. Zhang, Y.X. Chen, Z. Guo, H.L. Liu, D.P. Wang, X.J. Huang, Bioinspired multifunctional hetero-hierarchical micro/nanostructure tetragonal array with self-cleaning, anticorrosion, and concentrators for the SERS detection, ACS applied materials & interfaces, 5 (2013) 10633-10642.

[31] H. Zhao, K.Y. Law, V. Sambhy, Fabrication, surface properties, and origin of superoleophobicity for a model textured surface, Langmuir : the ACS journal of surfaces and colloids, 27 (2011) 5927-5935.

[32] Y. Wu, Y. Wang, H. Liu, Y. Liu, L. Guo, D. Jia, J. Ouyang, Y. Zhou, The fabrication and hydrophobic property of micro-nano patterned surface on magnesium alloy using combined sparking sculpture and etching route, Applied Surface Science, 389 (2016) 80-87.

[33] Y. Liu, X. Yin, J. Zhang, S. Yu, Z. Han, L. Ren, A electro-deposition process for fabrication of biomimetic super-hydrophobic surface and its corrosion resistance on magnesium alloy, Electrochimica Acta, 125 (2014) 395-403.

[34] Y. Liu, S. Li, J. Zhang, Y. Wang, Z. Han, L. Ren, Fabrication of biomimetic superhydrophobic surface with controlled adhesion by electrodeposition, Chemical Engineering Journal, 248 (2014) 440-447.

[35] Z. Chen, L. Hao, C. Chen, A fast electrodeposition method for fabrication of lanthanum superhydrophobic surface with hierarchical micro-nanostructures, Colloids and Surfaces A: Physicochemical and Engineering Aspects, 401 (2012) 1-7.

[36] F. Su, K. Yao, C. Liu, P. Huang, Rapid Fabrication of Corrosion Resistant and Superhydrophobic Cobalt Coating by a One-Step Electrodeposition, Journal of the Electrochemical Society, 160 (2013) D593-D599.

[37] J.M. Lee, K.M. Bae, K.K. Jung, J.H. Jeong, J.S. Ko, Creation of microstructured surfaces using Cu–Ni composite electrodeposition and their application to superhydrophobic surfaces, Applied Surface Science, 289 (2014) 14-20.

[38] P. Sivasakthi, G.R. Bapu, M. Chandrasekaran, S. Sreejakumari, Synthesis of a super-hydrophobic Ni–ITO nanocomposite with pine-cone and spherical shaped micro-nanoarchitectures by pulse electrodeposition and its electrocatalytic application, RSC Advances, 6 (2016) 44766-44773.

[39] V. Torabinejad, M. Aliofkhazraei, A.S. Rouhaghdam, M.H. Allahyarzadeh, The hydrophobicity of Ni–Fe alloy electrodeposits obtained at different current densities, Transactions of the Institute of Metal Finishing, 95 (2017) 190-196.

[40] T. Ishizaki, Y. Masuda, M. Sakamoto, Corrosion resistance and durability of superhydrophobic surface formed on magnesium alloy coated with nanostructured cerium oxide film and fluoroalkylsilane molecules in corrosive NaCl aqueous solution, Langmuir the ACS Journal of Surfaces & Colloids, 27 (2011) 4780-4788.

[41] W. Xiao, Z. Huang, Z. He, Tuning the wettability on La0.7Sr0.3MnO3 coatings from superhydrophilicity to superhydrophobicity by hierarchical microstructure, Applied Physics Letters, 89 (2006) 165.

[42] D. Landolt, A. Marlot, Microstructure and composition of pulse-plated metals and alloys, Surface and Coatings Technology, 169 (2003) 8-13.

[43] S.O. Pagotto, C.M. de Alvarenga Freire, M. Ballester, Zn–Ni alloy deposits obtained by continuous and

ACCEPTED MANUSCRIPT

pulsed electrodeposition processes, Surface and Coatings Technology, 122 (1999) 10-13.
[44] R. Choo, J. Toguri, A. El-Sherik, U. Erb, Mass transfer and electrocrystallization analyses of nanocrystalline nickel production by pulse plating, Journal of Applied Electrochemistry, 25 (1995) 384-403.
[45] C. Gu, J. Tu, One-step fabrication of nanostructured Ni film with lotus effect from deep eutectic solvent, Langmuir : the ACS journal of surfaces and colloids, 27 (2011) 10132-10140.
[46] R.S. Bajwa, Z. Khan, V. Bakolas, W. Braun, Water-Lubricated Ni-Based Composite (Ni–Al 2 O 3 , Ni–SiC and Ni–ZrO 2 ) Thin Film Coatings for Industrial Applications, Acta Metallurgica Sinica, 29 (2016) 8-16.
[47] M.H. Allahyarzadeh, M. Aliofkhazraei, A.R.S. Rouhaghdam, V. Torabinejad, Structure and wettability of pulsed electrodeposited Ni-W-Cu-(α-alumina) nanocomposite, Surface & Coatings Technology, 307 (2016) 525-533.
[48] G.T. Chandrappa, N. Steunou, J. Livage, Materials chemistry: macroporous crystalline vanadium oxide foam, Nature, 416 (2002) 702.
[49] M.A. Osman, U.W. Suter, Surface treatment of calcite with fatty acids: structure and properties of the organic monolayer, Chemistry of materials, 14 (2002) 4408-4415.
[50] F. Robert, Coming to an unsticky end, Nature, 368 (1994) 16.
[51] T.G. Raja, K. Jeyasubramanian, Tuning the superhydrophobicity of magnesium stearate decorated ZnO porous structures for self-cleaning urinary coatings, Applied Surface Science, 423 (2017) 293-304.
[52] J.C. Bird, R. Dhiman, H.-M. Kwon, K.K. Varanasi, Reducing the contact time of a bouncing drop, Nature, 503 (2013) 385-388.
[53] Y. Yang, Y. Cheng, Electrolytic deposition of Ni–Co–SiC nano-coating for erosion-enhanced corrosion of carbon steel pipes in oilsand slurry, Surface and coatings technology, 205 (2011) 3198-3204.

ACCEPTED MANUSCRIPT

ACCEPTED MANUSCRIPT

**Highlights**

- Pulse electrodeposition of superhydrophobic surface with rare earth electrolyte.
- Pulse frequency has a great influence on the formation and morphology of deposits.
- The as-prepared surfaces are superhydrophobic without further modification.
- This method is time-saving and the superhydrophobic surface is long-term stable.

ACCEPTED MANUSCRIPT